IL NUOVO CIMENTO **43 C** (2020) 114
DOI 10.1393/ncc/i2020-20114-4

COMMUNICATIONS: SIF Congress 2019

First-principles approach to novel 2D magnets

D. AMOROSO

National Research Council CNR-SPIN, c/o Università degli Studi G. D'Annunzio I-66100 Chieti, Italy

received 21 February 2020

Summary. — There is an increasing interest towards long-range magnetic order in two-dimensional materials (such as CrI_3 and $CrGeTe_3$), both from the fundamental and the applicative point of view. As well known, functional properties can change when scaling down the dimensionality of a system. Particularly, this applies to magnetic materials, which must display anisotropic interactions in order to preserve a magnetic ordering in the two-dimensional space, as follows from the Mermin-Wagner theorem. In the aim of finding new appealing systems hosting low-dimensional magnetism, in this work we carry out an investigation based on first-principles calculations on the nickel dihalides NiX_2 (X = Cl, Br, I) class of materials, going from standard analysis of structural and electronic properties to the magnetic properties, in terms of magnetic moments and Heisenberg exchange interaction. Some of the considered materials show exchange coupling constants strongly dependent on spin-orbit coupling, leading to the expectation that anisotropic contribution to the magnetic interaction should play an impotant role in the magnetic properties of these systems.

1. – Introduction

The global tendency towards miniaturization and efficiency improvements of microelectronic devices has boosted, in recent years, the interest in the understanding and developments of low-dimensional materials. In particular, the challenge concerns the finding of materials able to host magnetic properties when scaling the dimensionality from 3D to 2D. In fact, one- or two-dimensional systems with isotropic magnetic interactions cannot order (neither ferromagnetically nor antiferromagnetically) [1]. Magnetic anisotropy can remove this restriction, and allows the realization of long-range magnetic ordering in two-dimensional systems. This behaviour has been recently found in $CrGeTe_3$ and CrI_3 van der Waals crystals [2]; indeed, in 2017, Gong and co-workers reported ferromagnetic ordering in pristine $CrGeTe_3$ bilayer [3], while Huang *et al.* showed Ising-type ferromagnetic order in one-layer-thick CrI_3, and layer-dependent magnetic phases [4]. The comprehensive theoretical work of Xu and co-workers [5] provides then an insight for the understanding of the observed 2D ferromagnetic behaviour, going through a deep

analysis of the magnetic anisotropies in these systems. In particular, they reported that such anisotropies arise from the spin-orbit coupling (SOC) of the heavy ligand element.

Inspired by such findings, we decided to approach by means of first-principles calculations the investigation of a similar class of van der Waals materials, the nickel dihalides. Particularly, the focus will be on $NiCl_2$, $NiBr_2$ and NiI_2 monolayers. Bulk $NiCl_2$, $NiBr_2$ and NiI_2 are in fact known to undergo magnetic phase transitions; in particular, at low temperature, $NiCl_2$ is found to exhibit an antiferromagnetic order, due to antiferromagnetic intralayer coupling between ferromagnetic layers, while $NiBr_2$ and NiI_2 are ordered following more complex helimagnetic spin structures (see ref. [6] and references therein). Nevertheless, the experimental characterization of their single 2D layers has not been performed yet, and theoretical studies still remain limited. In particular, in previous density-functional-theory–based works, the SOC contribution to the magnetic exchange has not been fully considered. Rather, we show that it should be better taken into account, for a proper characterization of the magnetic properties.

2. – Technical details

Ab initio calculations have been performed within the density functional theory (DFT) using the projector-augmented wave methods, as implemented in the VASP code [7, 8]. The exchange-correlation potential was evaluated within the generalized gradient approximation (GGA) using the Perdew-Burke-Erzenhof (PBE) functional [9]. The energy cutoff for the expansion of the electronic wave functions has been fixed to 600 eV for $NiCl_2$ and $NiBr_2$, and to 500 eV for NiI_2.

First, we determined the DFT structure of the monolayer for the three materials, performing relaxation of the atomic positions fixing various in-plane lattice parameters a; we performed calculations for the primitive cell using a $18 \times 18 \times 1$ k-points mesh for the sampling of the Brillouin zone, adopting a ferromagnetic (FM) spin configuration within standard collinear calculations.

For the evaluation of the magnetic exchange coupling and the magnetocrystalline anisotropy, the SOC was also introduced along with the U-correction on the localized $3d$ electrons of Ni atoms; here we report results for an effective parameter, $U_{eff} = 2\,\text{eV}$, within the Dudarev approach [10, 11]. We also performed calculations employing $U = 1.8\,\text{eV}$ and $J = 0.8\,\text{eV}$ within the Liechtenstein approach [12], that leads to similar results. In particular, here we evaluate an effective nearest-neighbours magnetic exchange coupling, performing energy calculations for ferromagnetically and "striped"-wise antiferromagnetically ordered supercells of size $3 \times 2 \times 1$ (fig. 1(c), (d)). In all cases, the length of the out-of-plane lattice parameter, perpendicular to the monolayer plane, was fixed to 20.8 Å.

3. – Structural properties

In the dihalides family the transition metal cations, here Ni atoms, are arranged in a triangular net, as shown in fig. 1(a). In particular, a single layer contains edge-shared NiX_6 octahedra (fig. 1(b)) with same Ni-Ni and Ni-X distances, which preserve spatial inversion symmetry. The octahedron exhibits in turns a trigonal distortion with alternating shorter and longer X-X distances: the anion-anion distance along the shared edge is shorter than along the other direction; the latter being the same as the nearest-neighbour Ni-Ni distance, which in turn is equal to the in-plane lattice parameter a. This trigonal structure analysed for the three NiX_2 monolayers is usually called 1-T crystal structure [13] and has D_{3d} symmetry and $P\bar{3}m1$ space group. The calculated structural

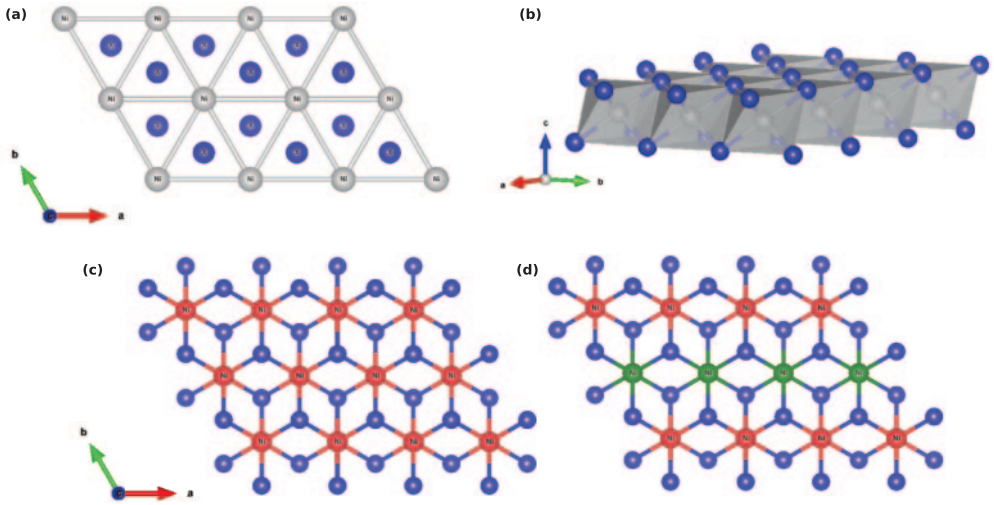

Fig. 1. – Crystal structure of nickel dihalides (NiX_2) monolayer; halide (X) is in blue color. (a) Top view highlighting the triangular net of Ni atoms. (b) Side view highlighting the MX_6 edge-shared octahedra. (c)–(d) Schematic representation of the FM and AFM ordered 3×2×1 supercell used for the energy mapping to evaluate the effective magnetic exchange coupling between first-neighbour Ni atoms. Red and green atoms represent up and down spins, respectively.

parameters are reported in table I, and agree with the experimental bulk data [6] within the known DFT-PBE error [14]. The M-X-M bond angle is about 93° in all the three systems.

4. – Electronic properties

Nickel, with d^8 electronic configuration, is a divalent cation in all the three compounds. The total magnetic moment per unit cell is $2\mu_B$, with a large contribution arising from the Ni site. Nevertheless, the halogens also develop a local magnetic moment and show a significant ferromagnetic spin-polarization, as reported in table I. In closer detail, the

TABLE I. – *Various calculated properties for the three dihalide monolayers. First column: structural parameters as obtained from calculation without SOC and with $U_{eff} = 0\,eV$; in particular the lattice constant a, the Ni-X and X-X distances. Second column: magnetic moments calculated on Ni and halide (X) atoms. Third column: Magnetocrystalline anisotropy energy for the magnetic moments pointing out-of-plane (z) vs. in-plane (x) direction. Fourth column: Effective magnetic exchange coupling between first-neighbour distant Ni atoms from energy mapping on a FM and stripy-AFM spin configurations illustrated in fig. 1(c), (d), without and with SOC inclusion in the DFT-calculations. Both MAE and $J_{iso}^{1\,eff}$ calculations include DFT-U correction with $U_{eff} = 2\,eV$.*

	Distances (Å)			MM/μ_B		MAE (meV)	$J_{iso}^{1\,eff}$ (meV)	
	a	Ni-X	X-X	Ni	X	FM_z-FM_x	no SOC	w SOC
$NiCl_2$	3.49	2.40	3.49–3.30	1.53	0.19	0.00	−5.25	−5.26
$NiBr_2$	3.69	2.55	3.69–3.52	1.46	0.21	+0.04	−5.70	−6.28
NiI_2	3.96	2.74	3.96–3.78	1.35	0.22	−0.13	−6.48	−7.24

magnetic moment on the metal cation decreases with the increasing atomic number Z of the halide atom, and vice versa for the induced moment on the anions (Cl $\rightarrow$ Br $\rightarrow$ I), in agreement with previous results [15].

Moreover, the crystal field related to the octahedral atomic coordination splits the $3d$ orbital of the metal atom into higher energy e_g and lower energy t_{2g} states, leading thus to unoccupied e_g minority spin bands; the t_{2g} states are in fact fully occupied, while the two remanent electrons occupy the e_g only in one spin channel. This produces the opening of a band gap, making $NiCl_2$, $NiBr_2$ and NiI_2 all semiconductors. The calculated density of states (DOS) reported in fig. 2 displays this semiconductive character. In particular, the gap decreases when going from $NiCl_2$ to NiI_2. This could be ascribed to the different

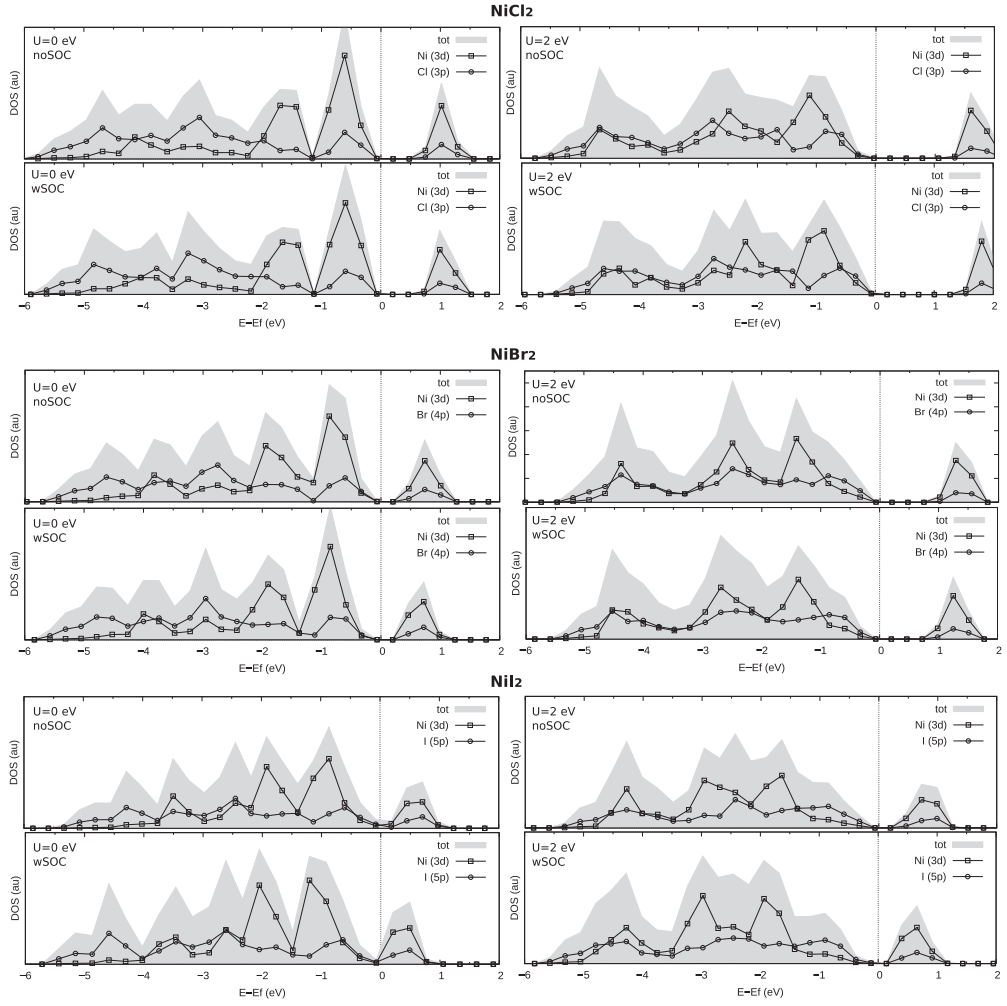

Fig. 2. – Atom-resolved density of states (DOS) without and with SOC for $NiCl_2$, $NiBr_2$ and NiI_2. Left and right panels show DOS from calculations with $U_{eff} = 0\,\text{eV}$ and $U_{eff} = 2\,\text{eV}$, respectively. d states from nickel are represented in open squares, whereas p states from the halides are shown in open circles.

electronegativity of the three halogens, being Cl (I) atom the most (least) electronegative and to the hybridization between Ni and anion p states, which mainly form the top of the valence bands. The interactions can in fact change when going from localized $3p$ orbitals of Cl to the broader $5p$ orbitals of I.

It is also noteworthy the effect of the SOC inclusion on the electronic band gap. In fact, the spin-orbit coupling produces a small reduction of the gap, mainly in $NiBr_2$ and NiI_2, the SOC effect increasing with the Z of the halogen atoms. The effect of such reduction is far more critical for the latter system: the already narrow gap obtained by collinear DFT calculations without U-correction, is almost closed when introducing the SOC. The introduction of a small U allows to preserve an energy gap and a clear semiconductive character of the systems, which is of particular importance when studying their magnetic properties. The increase of the gap operated by the U in all the three systems, without and with SOC, is evident in fig. 2.

5. – Magnetic properties

As mentioned in the introductory section, a 2D material, such as the NiX_2 monolayers, can present an ordered magnetic phase if the magnetic interaction shows some anisotropic behaviour. The spin-orbit coupling allows the interaction between the spin and lattice degrees of freedom in the systems, and, in turn, the emergence of eventual anisotropies. Energy mapping for the evaluation of the magnetic exchange interactions performed via collinear calculations (without SOC) in fact allows only to determine the relative orientation of spins in a magnetic system, but does not allow to access the absolute spin orientation and direction in space [16]; this then makes the introduction of SOC in DFT-calculations of fundamental importance.

By doing this, a first accessible meaningful quantity is indeed the magnetocrystalline anisotropy (MAE), which is a global measure of eventual preferred spin orientations in space, and thus reveals isotropic or anisotropic character of the magnetic interaction. The simplest way to access this information is then to evaluate the energy difference between ferromagnetically ordered spins, but alternately directed along the z-direction, which is the out-of-plane direction in our monolayer systems, and along the in-plane x- or y-direction. The resulting MAE in $NiCl_2$, $NiBr_2$ and NiI_2 is reported in table I: $NiCl_2$ does not display preferred spatial orientations of spins, suggesting that it likely behaves as an isotropic, Heisenberg-like, system. On the other hand, $NiBr_2$ and NiI_2 display a non-zero MAE, which ensures an anisotropic behavior. In particular, NiI_2 hosts a much stronger anisotropy. These results also show that the spin-lattice coupling is stronger in the systems with heavy halide ligands (Cl $\rightarrow$ Br $\rightarrow$ I), as expected from previous findings in CrI_3 and $CrGeTe_3$ [5].

In order to further check the relevance of the SOC in the magnetic exchange properties of these three systems, we evaluated an effective magnetic interaction between nearest-neighbour Ni-Ni atoms, J_{iso}^{1eff}, performing energy calculations without and with SOC on two different magnetically ordered structures, a FM and an AFM structure as illustrated in fig. 1(c), (d). We then extracted the exchange parameter by modelling the spin-spin interaction via a classical Heisenberg Hamiltonian: $H_{spin} = \frac{1}{2} J_{iso}^{1eff} \sum_{i \neq j} \vec{S_i} \cdot \vec{S_j}$. J_{iso}^{1eff} is the scalar exchange coupling between near-neighbour spins ($\vec{S_i}$, $\vec{S_j}$); the extracted effective exchange contains the influence from the interaction between second-neighbours (J_2) to the first-neighbour (J_1) exchange. The results, reported in table I, show a ferromagnetic interaction between nearest-neighbour Ni atoms and confirm our expecta-

tion: collinear calculations (without SOC) underestimate the magnetic exchange between nearest-neighbour magnetic sites in $NiBr_2$ and NiI_2; the error increases with increasing SOC of the halide ligand, also in line with the above-discussed MAE trend.

Our findings point out two main evidences: i) $NiBr_2$ and NiI_2 clearly show the required magnetic anisotropy for the realization of low-dimensional magnetic order; ii) the strong SOC effect in the estimate of some magnetic properties suggests, from a methodology point of view, that these systems have to be investigated going beyond standard and simplified energy mapping, which could lead to inaccurate and limited description of their magnetic properties, as in previous theoretical works [13,15]. Moreover, to properly define the magnetic ground state of these nickel dihalides systems, the extension to the interaction beyond nearest-neighbours can be of significant relevance [17]. As introduced in the description of the structural properties of NiX_2, the transition metals in the dihalide systems adopt a triangular net, rather then a honeycomb net as in the trihalides, like CrI_3. This triangular lattice of magnetic sites can also introduce magnetic frustration when antiferromagnetic (AFM) interactions occur. Particularly, the interaction betweeen third neighbour magnetic sites, if AFM, could be strong enough to compete with the FM first-neighbours interaction, being the exchange coupling mediated by another transition metal cation.

6. – Summary

In summary, in this paper we investigated the evolution of some structural, electronic and magnetic properties in the monolayer of the three nickel dihalides $NiCl_2$, $NiBr_2$ and NiI_2 by means of first-principles calculations, in order to explore possible low-dimensional magnetism. Our DFT-results show such a possibility in $NiBr_2$ and NiI_2 systems. Moreover, we highlight here the necessity to improve the modelling of these systems by considering the effect of spin-orbit coupling and the next nearest-neighbour interactions in order to have better insights on the understanding and prediction of their magnetic properties.

* * *

The author acknowledges her collaborators and colleagues, Paolo Barone and Silvia Picozzi.

REFERENCES

[1] Mermin N. D. and Wagner H., *Phys. Rev. Lett.*, **17** (1966) 1133.
[2] *2D magnetism gets hot*, *Nat. Nanotechnol.*, **13** (2018) 269 (Editorial).
[3] Cong C. *et al.*, *Nature*, **546** (2017) 265.
[4] Huang B. *et al.*, *Nature*, **546** (2017) 270.
[5] Xu C. *et al.*, *npj Comput. Mater.*, **4** (2018) 57.
[6] McGuire M. A., *Crystals*, **7** (2017) 121.
[7] Kresse G. and Furthmüller H., *Phys. Rev. B*, **54** (1996) 11169.
[8] VASP official website, `http://cms.mpi.univie.ac.at/vasp`.
[9] Perdew J. P., Burke K. and Ernzerhof M., *Phys. Rev. Lett.*, **77** (1996) 3865.
[10] Rohrbach A. *et al.*, *J. Phys.: Condens. Matter*, **15** (2003) 979.

[11] Dudarev A. *et al.*, *Phys. Rev. B*, **57** (1998) 1505.
[12] Liechtenstein A. *et al.*, *Phys. Rev. B*, **52** (1995) R5467(R).
[13] Kulish V. V. and Huang W., *J. Mater. Chem.*, **5** (2017) 8734.
[14] Haas P., Tran F. and Blaha P., *Phys. Rev. B*, **79** (2009) 085104.
[15] Botana A. S. and Norman M. R., *Phys. Rev. Mater.*, **3** (2019) 044001.
[16] Xiang H. *et al.*, *Dalton Trans.*, **42** (2013) 823.
[17] Amoroso D., Barone P. and Picozzi S., arXiv:2005.02714 [cond-mat.mtrl-sci] (2020).